

## Multifractal Analysis with the Probability Density Function at the Three-Dimensional Anderson Transition

Alberto Rodriguez,<sup>1,2,\*</sup> Louella J. Vasquez,<sup>1</sup> and Rudolf A. Römer<sup>1</sup>

<sup>1</sup>*Department of Physics and Centre for Scientific Computing, University of Warwick, Coventry, CV4 7AL, United Kingdom*

<sup>2</sup>*Departamento de Física Fundamental, Universidad de Salamanca, 37008 Salamanca, Spain*

(Received 8 December 2008; published 13 March 2009)

The probability density function (PDF) for critical wave function amplitudes is studied in the three-dimensional Anderson model. We present a formal expression between the PDF and the multifractal spectrum  $f(\alpha)$  in which the role of finite-size corrections is properly analyzed. We show the non-Gaussian nature and the existence of a symmetry relation in the PDF. From the PDF, we extract information about  $f(\alpha)$  at criticality such as the presence of negative fractal dimensions and the possible existence of termination points. A PDF-based multifractal analysis is shown to be a valid alternative to the standard approach based on the scaling of inverse participation ratios.

DOI: 10.1103/PhysRevLett.102.106406

PACS numbers: 71.30.+h, 05.45.Df, 72.15.Rn

The fluctuations and correlations of wave amplitudes are of primary importance for the understanding of many classical and quantum systems. This is arguably most pronounced in the physics of Anderson localization [1]. Here, recent advancements in theory [2,3], experiments in classical [4] and quantum waves [5,6], as well as numerical methods [7] have led to unprecedented insights into the nature of the localization-delocalization transition. In contrast to the weak- or strong-disorder limits where the description of nearly extended or strongly localized states is well known, e.g., from random matrix theory [8], the intensity distribution at the metal-insulator transition is more involved due to the multifractal nature of the states [1,9,10]. The possibility of carrying out a multifractal analysis directly from the raw statistics of intensities  $|\psi|^2$ , i.e., the probability density function (PDF), is especially interesting since their distributions can be measured experimentally in classical [4] and quantum [5,11,12] experiments. However, the numerical relation between the PDF and the multifractal spectrum  $f(\alpha)$  has not been completely elucidated. In this Letter we show how to obtain the multifractal spectrum based on the PDF. The PDF-to- $f(\alpha)$  connection is a numerically much simpler procedure than the usual scaling of  $q$  moments of  $|\psi|^2$  [13]. Furthermore, it yields direct understanding of physical properties at criticality, such as the existence of a symmetry relation, the observation of negative fractal dimensions and the physical meaning of the possible appearance of termination points. We apply the PDF-based approach to the three-dimensional Anderson model within the Gaussian orthogonal ensemble, using a large number of critical states at  $E = 0$  and very large system sizes up to  $L^3 = 240^3$  [7].

At criticality, the  $|\psi|^2$  distribution has the scaling form

$$\mathcal{P}_L(|\psi|^2) \sim (1/|\psi|^2)L^{f(-\ln|\psi|^2/\ln L)-d}. \quad (1)$$

In terms of the variable  $\alpha \equiv -\ln|\psi|^2/\ln L$ , the PDF is  $\mathcal{P}_L(\alpha) \sim L^{f(\alpha)-d}$ , where  $f(\alpha)$  is the multifractal spectrum,

i.e., the fractal dimensions of the different  $\alpha$  sets made up of the points where  $|\psi_i|^2 = L^{-\alpha}$ . The  $f(\alpha)$  spectrum is usually constructed by a Legendre transformation [13] of the scaling exponents  $\tau(q)$  for the generalized inverse participation ratios (GIPR)  $L^d \langle |\psi_i|^{2q} \rangle \sim L^{-\tau(q)}$  [2,3,7,14].

The relation (1) between  $\mathcal{P}_L(\alpha)$  and  $f(\alpha)$  suggests a complete characterization of multifractality directly from the PDF. The proportionality in (1) contains an  $L$  dependence which can be naively included as

$$\mathcal{P}_L(\alpha) = \mathcal{P}_L(\alpha_0)L^{f(\alpha)-d}, \quad (2)$$

where  $\alpha_0$  is the position of the maximum of the multifractal spectrum,  $f(\alpha_0) = d$ . Furthermore, since  $f(\alpha) < d$  for all  $\alpha \neq \alpha_0$ , we see that  $\mathcal{P}_L(\alpha_0)$  corresponds in fact to the maximum value of the PDF itself. Hence  $\alpha_0$  can be easily obtained numerically. As for  $f(\alpha)$ , the value of  $\alpha_0$  obtained from the PDF must be  $L$  invariant at criticality, as we show in Fig. 1. The estimation for  $\alpha_0 = 4.027 \pm 0.016$  from the PDF is in agreement with that obtained from GIPR scaling [7],  $\alpha_0 \in [4.024, 4.030]$ . From the normalization condition we find  $\mathcal{P}_L(\alpha_0) = (\int_0^\infty L^{f(\alpha)-d} d\alpha)^{-1}$ . Using the saddle point method, justified in the limit of large  $L$ , we compute  $\mathcal{P}_L(\alpha_0) \sim \sqrt{\ln L}$ , which holds very well even for small  $L$  as shown in Fig. 1(a). From the PDF for fixed  $L$  the multifractal spectrum is hence straightforwardly obtained from (2) as  $f(\alpha) = d + \ln[\mathcal{P}_L(\alpha)/\mathcal{P}_L(\alpha_0)]/\ln L$ . Alternatively, if  $f(\alpha)$  is known, the PDF can be easily generated. We find excellent agreement between the singularity spectrum obtained from the PDF for  $L = 30, \dots, 240$  and the one obtained from the more involved box-size scaling of the GIPR [7]. It must be noted that  $\mathcal{P}_L(\alpha)$  is always system-size dependent, and it is through the  $f(\alpha)$  spectrum that all PDFs for different  $L$  collapse onto the same function; cf. Fig. 1(b). Thus the  $f(\alpha)$  can also be understood as the natural scale-invariant distribution at criticality.

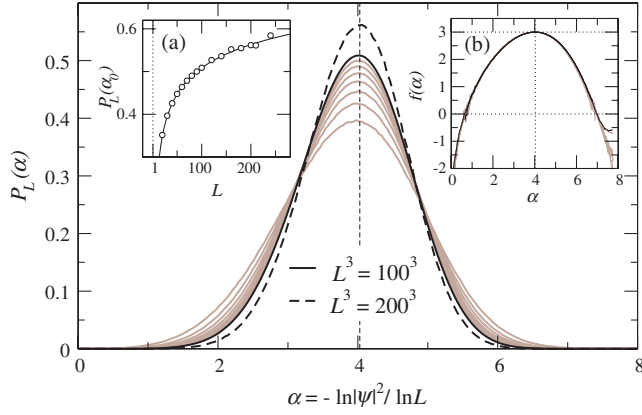


FIG. 1 (color online). PDF at criticality for  $\Delta\alpha = 0.04$ . The gray lines correspond to  $L$  from 30 (bottom) to 90 (top). Standard deviations are within the line width. For  $L \leq 100$  and  $L > 100$  we average over  $5 \times 10^4$  and 100 states, respectively. The vertical dashed line marks the mean value for  $\alpha_0 = 4.027 \pm 0.016$  using  $L$  from 50 to 200. Inset (a) shows  $\mathcal{P}_L(\alpha_0)$  vs  $L$ . Standard deviations are contained within symbol size. The solid line is the fit  $a \ln(L/l)^b$ , with  $a = 0.297 \pm 0.002$ ,  $b = 0.490 \pm 0.005$ . Inset (b) shows the collapse of all the PDF from  $L = 30$  to 240 onto the  $f(\alpha)$ .

In order to minimize finite-size effects, we can also determine  $f(\alpha)$  from the PDF using system-size scaling. We note that for a given  $L$  the number of points per wave function with  $\alpha \in [\alpha - \Delta\alpha/2, \alpha + \Delta\alpha/2]$  is  $\mathcal{N}_L(\alpha) \equiv L^d \mathcal{P}_L(\alpha) \Delta\alpha$ . Hence the following normalized volume of the  $\alpha$  set  $\tilde{\mathcal{N}}_L(\alpha) \equiv L^d \mathcal{P}_L(\alpha) / \mathcal{P}_L(\alpha_0)$  obeying

$$\tilde{\mathcal{N}}_L(\alpha) = L^{f(\alpha)}, \quad (3)$$

can be used to extract  $f(\alpha)$  from a series of systems with different  $L$ . In Fig. 2 we compare the multifractal spectrum obtained using PDF scaling (3) with the one from GIPR scaling [7] for  $L \in [20, 100]$  and having  $5 \times 10^4$  critical states for each size. We find very good agreement between both, as well as between the numerical PDFs and those generated from the GIPR  $f(\alpha)$  [Fig. 2(a)].

Numerically, the PDF is approximated by

$$\mathcal{P}_L(\alpha) \equiv_{\Delta\alpha \rightarrow 0} \langle \theta(\Delta\alpha/2 - |\alpha + \ln|\psi_i|^2 / \ln L|) \rangle / \Delta\alpha, \quad (4)$$

where  $\theta$  is the Heaviside step function and  $\langle \cdot \rangle$  involves an average over the volume of the system and all realizations of disorder. To minimize the uncertainty in the small  $|\psi_i|^2$ , which becomes greatly enhanced in terms of  $\alpha(|\psi_i|^2)$ , the amplitudes used for the histogram are those obtained from a coarse-graining procedure of the state using boxes of linear size  $l = 5$ . Therefore the system size in all equations is the *effective* system size  $L/l$ . The uncertainty of the PDF value is estimated from the usual standard deviation for a counting process as  $\sigma_{\mathcal{P}_L(\alpha)} = \sqrt{\mathcal{P}_L(\alpha) / N_w L^d \Delta\alpha}$ , where  $N_w$  is the total number of states in the average, and for the  $\alpha$  values a constant  $\sigma_\alpha = \Delta\alpha/3$  is assigned. This proce-

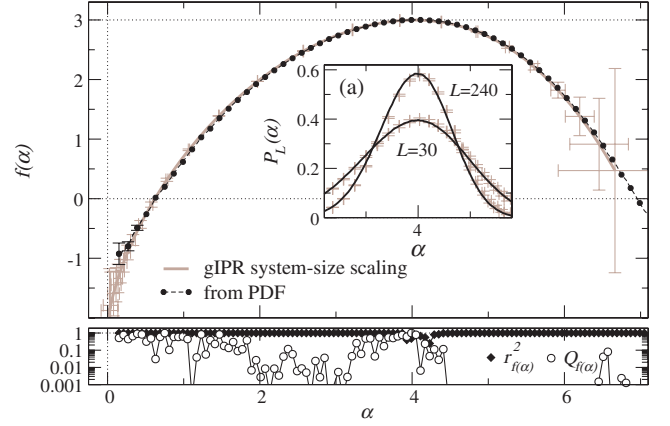


FIG. 2 (color online).  $f(\alpha)$  obtained from system-size scaling of the PDF and the GIPR, for  $L \in [20, 100]$ . Only one every second symbol is shown for clarity. Standard deviations are within symbol size when not shown. The inset shows the numerical PDF (black) and the PDF calculated from the GIPR  $f(\alpha)$  (gray). The bottom panel gives the linear correlation coefficient  $r^2$  and quality-of-fit parameter  $Q$  for the  $f(\alpha)$  obtained from the log-log linear fits of Eq. (3).

cedure assumes uncorrelated  $\alpha$ 's and hence  $|\psi|^2$ 's; this is only true between different disorder realizations, but not necessarily within each state. Hence the errors of the PDF are probably somewhat underestimated and the small uncertainty of the  $f(\alpha)$ -values obtained from PDF scaling in Fig. 2 must be interpreted carefully. There also exists another source of error difficult to quantify, namely, how much the histogram for finite  $\Delta\alpha$  deviates from the real PDF when  $\Delta\alpha \rightarrow 0$ . In spite of this, the PDF method is easy to implement numerically and hence a valid alternative to the more demanding GIPR scaling techniques.

*Symmetry relation for the PDF.*—The symmetry relation,  $f(2d - \alpha) = f(\alpha) + d - \alpha$  [2] for  $L \rightarrow \infty$ , implies the existence of a symmetry for the PDF which should hold for large enough system sizes,

$$\mathcal{P}_L(2d - \alpha) = L^{d-\alpha} \mathcal{P}_L(\alpha). \quad (5)$$

In terms of the wave function amplitudes, Eq. (5) reads  $\mathcal{P}_L(L^{-2d}/|\psi|^2) = (L^d|\psi|^2)^3 \mathcal{P}_L(|\psi|^2)$ . The latter relation establishes that at criticality the distribution in the interval  $L^{-2d} < |\psi|^2 \leq L^{-d}$  is indeed determined by the PDF in the region  $L^{-d} \leq |\psi|^2 < 1$ . We carry out a numerical check of the symmetry relation (5) by evaluating  $\delta\mathcal{P}_L(\alpha) = \mathcal{P}_L(\alpha) - L^{\alpha-d} \mathcal{P}_L(2d - \alpha)$  accounting for the distance between the original PDF and its symmetry-transformed counterpart at every  $\alpha$ , as well as the cumulative difference  $\delta(L) = \int_0^{2d} d\alpha |\delta\mathcal{P}_L(\alpha)|$ . The symmetry-transformed PDF for  $L = 100$  and the evolution of  $\delta\mathcal{P}_L(\alpha)$  for different  $L$  are shown in Fig. 3. We find that the symmetry relation is better satisfied as  $L$  increases [7], and the improvement can be roughly quantified as  $\delta(L) \sim L^{-0.545}$  as shown in Fig. 3(b).

*Non-Gaussian nature of the PDF.*—The parabolic approximation for  $f(\alpha)$  in  $d = 2 + \epsilon$ , [15] implies a

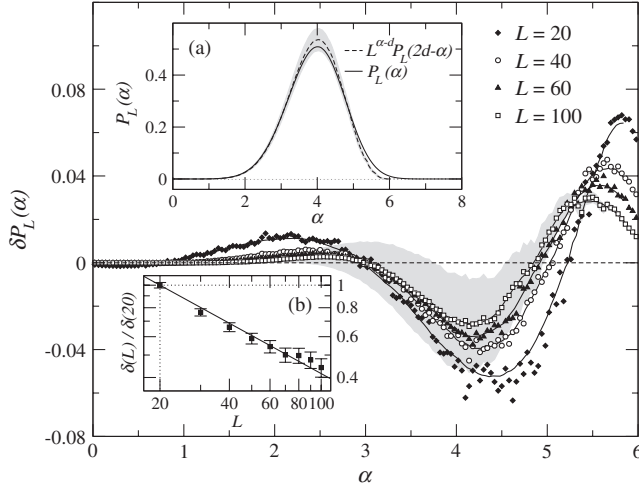


FIG. 3. Degree of symmetry of the PDF. The shaded region in the background marks the 66% confidence interval (c.i.) of the values for  $L = 100$ . The lines show the evolution in average for each  $L$ . The inset (a) displays the symmetry-transformed PDF for  $L = 100$  and its 95% c.i. (shaded region). The inset (b) shows a log-log plot of  $\delta(L)$  normalized to its maximum value. The solid line is a linear fit with slope  $b = -0.545 \pm 0.017$ .

Gaussian approximation (GA) for the PDF,  $\mathcal{P}_L^{\text{GA}}(\alpha) = \sqrt{\ln L / 4\pi\epsilon} L^{-[\alpha - (2+2\epsilon)]^2 / 4\epsilon}$ . The PDFs in Fig. 1 might indeed appear roughly Gaussian and in Fig. 4 we show Gaussian fits of the PDF for  $L = 100$ , obtained via a usual  $\chi^2$  minimization taking into account the uncertainties of the PDF values. However, the quality-of-fit parameter  $Q$ , which gives an indication on the reliability of the fit, is ridiculously small ( $Q < 10^{-300000}$ ). Since the standard deviations of the PDF values may have been slightly underestimated we also study how  $Q$  behaves when we intentionally increase the error bars by a factor  $n$ . As shown in

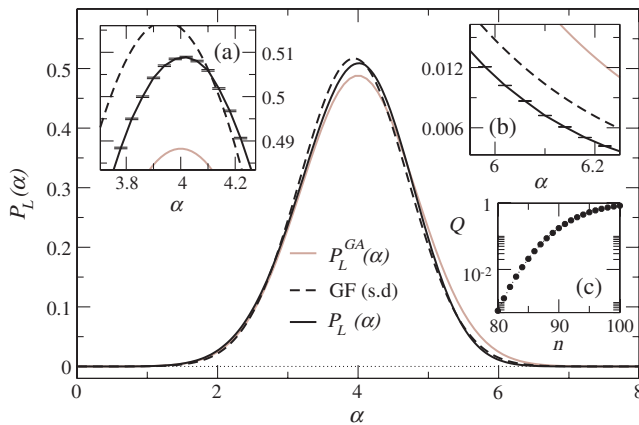


FIG. 4 (color online). Gaussian fit ( $\sqrt{a/\pi} e^{-a(x-b)^2}$ ) of the PDF for  $L^3 = 100^3$  (dashed line):  $a = 0.840 \pm 0.005$ ,  $b = 3.942 \pm 0.004$ ,  $Q < 10^{-300000}$ . The solid gray line shows the GA for  $\epsilon = 1$ . Insets (a) and (b) are blowups of the maximum and the right tail of the PDF. Inset (c) shows the quality-of-fit parameter  $Q$  when the standard deviation of the PDF points is multiplied by the factor  $n$ .

Fig. 4(c) one would have to go to unreasonable high values of  $n \sim 85$  to accept a Gaussian nature for the PDF as plausible. The deviation from  $\mathcal{P}_L^{\text{GA}}(\alpha)$  is also noticeable. Hence our statistical analysis confirms that the PDF is non-Gaussian in agreement with the observed nonparabolic nature of  $f(\alpha)$  at the 3D MIT [7].

*Rare events and their negative fractal dimensions.*—The volume of the  $\alpha$  set,  $\mathcal{N}_L(\alpha)$  for a given  $L$ , gives the number of points in the wave function with amplitudes in the range  $|\psi_i|^2 \in [L^{-\alpha-\Delta\alpha/2}, L^{-\alpha+\Delta\alpha/2}]$ . It scales with the system size as  $\mathcal{N}_L(\alpha) \sim \sqrt{\ln L} L^{f(\alpha)}$ . The negative values of  $f(\alpha)$  [7] correspond then to those  $\alpha$  sets whose volume decreases with  $L$  for large enough  $L$ . Physically, the negative fractal dimensions at small  $\alpha$  are caused by the so-called rare events containing localizedlike regions of anomalously high  $|\psi_i|^2$  at criticality. The probability of finding them likewise decreases with  $L$ . In Fig. 5, we show examples of rare eigenstates. Because of the finite-size term  $\sqrt{\ln L}$ , the threshold  $\alpha_-$  [where  $f(\alpha_-) = 0$ ], below which the decreasing behavior of  $\mathcal{N}_L(\alpha)$  with  $L$  is detected, will change with the system-size itself, and so the normalized volume (3) of the  $\alpha$  set must be used. In Fig. 6 we show the behavior of  $\tilde{\mathcal{N}}_L(\alpha)$  vs  $L$  for two values of  $\alpha$  corresponding to a positive and a negative fractal dimension. The decreasing of the volume of the  $\alpha$  set for  $f(\alpha) < 0$  is clearly observed from the PDF values. In Fig. 6(a) it is demonstrated how the normalized volume of the  $\alpha$  set becomes scale invariant at  $\alpha_-$  and thus  $\tilde{\mathcal{N}}_L(\alpha_-) = 1$ . The opposite tendencies with  $L$  at each side of  $\alpha_-$  can also be seen. The estimated value for  $\alpha_- \in [0.643, 0.675]$  from the PDF scaling agrees with the result obtained using the multifractal spectrum from GIPR scaling,  $\alpha_- = 0.626 \pm 0.028$  [7].

*Termination points in  $f(\alpha)$ .*—The fate of the  $f(\alpha)$  spectrum at  $\alpha = 0$  and  $\alpha = 2d$  is currently under debate in the literature [7,16] due to the emergence of singularities at

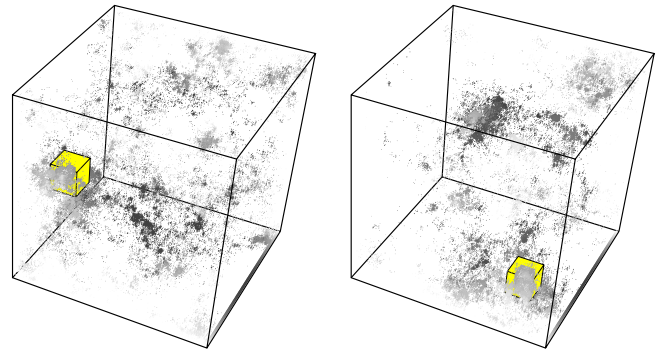


FIG. 5 (color online). Rare eigenstates for the 3D Anderson model ( $E = 0$ ,  $W_c = 16.5$ ) for  $L^3 = 100^3$ . The sites with probability  $|\psi_i|^2 > L^{-3}$  are shown as boxes with volume  $|\psi_i|^2 L^3$ . The gray scale distinguishes between different slices of the system along the axis into the page. The biggest boxes with black edges enclose the site with the maximum normalized amplitude:  $|\psi_i|^2 = 0.4484$  (left) and  $0.3617$  (right).

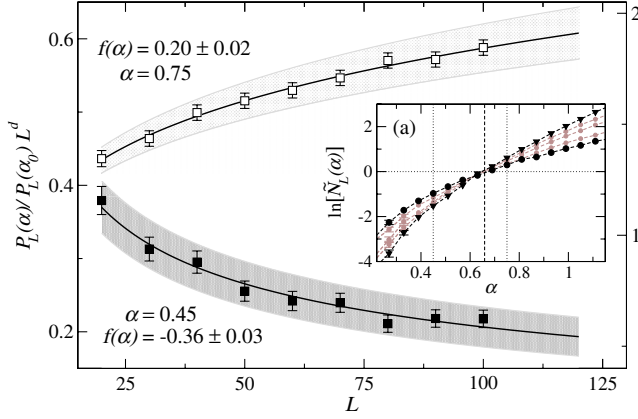


FIG. 6 (color online).  $\tilde{N}_L(\alpha)$  vs  $L$  for  $\alpha = 0.45$  (filled squares, left y axis) and  $0.75$  (open squares, right y axis). The solid lines are the  $L^{f(\alpha)}$  curves where  $f(\alpha)$  is obtained from the log-log linear fits of Eq. (3). The shaded regions mark the 66% c.i. of the  $L^{f(\alpha)}$  values. The inset shows  $\ln[\tilde{N}_L(\alpha)]$  vs  $\alpha$  for different  $L$  in the range [20 (black circle), 100 (black triangle)]. Standard deviations are within symbol size, whenever not shown. The vertical dashed line corresponds to the mean value of the crossing point  $\alpha_- = 0.659 \pm 0.008$ .

these points. At present, it is not clear whether  $f(\alpha)$  continues towards  $-\infty$  or terminates with finite values. The physical consequences of the divergence of  $f(\alpha)$  at those points are: (i)  $|\psi_i|^2 > L^{-2d}$  at criticality since  $2d$  would be an upper bound for  $\alpha$ , and (ii) the probability to find the most rare event, namely, the most extremely localized state ( $|\psi_{i_0}|^2 = 1$ , corresponding to  $\alpha = 0$ ), at the critical point must always be zero independently of the system-size [ $\mathcal{P}_L(0) = 0$ ]. In principle the PDF can be used to look for termination points (TP). However, a reliable analysis in the vicinity of  $\alpha = 0$  requires a huge number of disorder realizations; relying on the symmetry relation [2] a study around  $\alpha = 2d$  is more appropriate. For  $1 \ll \alpha < 2d$  and as long as there is a finite TP, the PDF admits the series expansion [17]

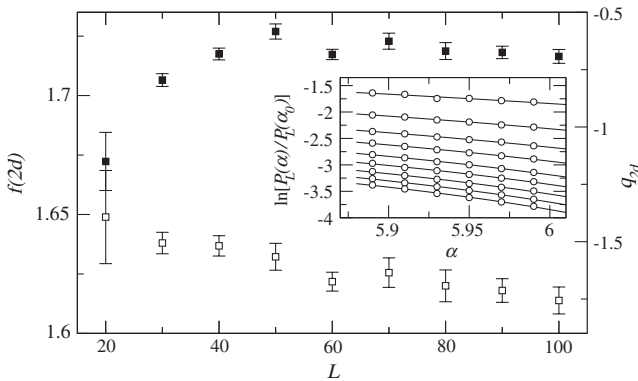


FIG. 7.  $f(2d)$  (filled squares, left y axis) and  $q_{2d} \equiv f'(\alpha)|_{\alpha=2d}$  (open squares, right y axis) as functions of system size. The inset shows the fits of Eq. (6) for different  $L$  from 20 (top) to 100 (bottom). Standard deviations are within symbol size.

$$\mathcal{P}_L(\alpha) \approx \mathcal{P}_L(\alpha_0)L^{f(2d)-d}[1 + q_{2d}(\alpha - 2d)\ln L], \quad (6)$$

where  $q_{2d} \equiv f'(\alpha)|_{\alpha=2d}$ . The existence of a finite TP at  $\alpha = 0$  requires  $f(2d)$  and  $q_{2d}$  to be  $L$  independent, for large enough  $L$ . In Fig. 7 we show the values of  $f(2d)$  and  $q_{2d}$  obtained for different  $L$ . The value of  $f(2d)$  seems to reach a saturation for large  $L$  although the numerical analysis cannot exclude a very slow decreasing tendency. A similar result is found for  $q_{2d}$ . Still larger  $L$  and more states are needed to decide the fate of  $f(\alpha)$  at 0 and  $2d$ .

In conclusion, we have shown here that a PDF-based study can be a valid companion approach to the standard multifractal analysis, giving complementary and new information about the critical properties of waves at Anderson-type transitions as well as offering a conceptually simpler viewpoint.

A. R. acknowledges financial support from the Spanish government (FIS2006-00716, MMA-A106/2007) and JCyL (SA052A07). R. A. R. gratefully acknowledges EPSRC (EP/C007042/1) for financial support.

\*Corresponding author.

A.Rodriguez-Gonzalez@warwick.ac.uk

- [1] F. Evers and A.D. Mirlin, Rev. Mod. Phys. **80**, 1355 (2008).
- [2] A. D. Mirlin, Y. V. Fyodorov, A. Mildenerger, and F. Evers, Phys. Rev. Lett. **97**, 046803 (2006).
- [3] H. Obuse, A. R. Subramaniam, A. Furusaki, I. A. Gruzberg, and A. W. W. Ludwig, Phys. Rev. Lett. **101**, 116802 (2008); F. Evers, A. Mildenerger, and A. D. Mirlin, *ibid.* **101**, 116803 (2008).
- [4] H. Hu *et al.*, Nature Phys. **4**, 945 (2008).
- [5] K. Hashimoto *et al.*, Phys. Rev. Lett. **101**, 256802 (2008).
- [6] G. Roati *et al.*, Nature (London) **453**, 895 (2008); J. Billy *et al.*, *ibid.* **453**, 891 (2008).
- [7] L. J. Vasquez, A. Rodriguez, and R. A. Römer, Phys. Rev. B **78**, 195106 (2008); A. Rodriguez, L. J. Vasquez, and R. A. Römer, *ibid.* **78**, 195107 (2008).
- [8] K. Müller, B. Mehlig, F. Milde, and M. Schreiber, Phys. Rev. Lett. **78**, 215 (1997).
- [9] H. Aoki, J. Phys. C **16**, L205 (1983).
- [10] J. J. Ludlam, S. N. Taraskin, S. R. Elliot, and D. A. Drabold, J. Phys. Condens. Matter **17**, L321 (2005).
- [11] M. Morgenstern, J. Klijn, C. Meyer, and R. Wiesendanger, Phys. Rev. Lett. **90**, 056804 (2003).
- [12] M. Morgenstern *et al.*, Phys. Rev. Lett. **89**, 136806 (2002).
- [13] M. Janssen, Int. J. Mod. Phys. B **8**, 943 (1994); Phys. Rep. **295**, 1 (1998).
- [14] F. Milde, R. A. Römer, and M. Schreiber, Phys. Rev. B **55**, 9463 (1997).
- [15] F. Wegner, Nucl. Phys. **B316**, 663 (1989).
- [16] H. Obuse, A. R. Subramaniam, A. Furusaki, I. A. Gruzberg, and A. W. W. Ludwig, Phys. Rev. Lett. **98**, 156802 (2007).
- [17] We assume that  $f'(\alpha)|_{\alpha=0}$  and  $f'(\alpha)|_{\alpha=2d}$  remain finite for finite  $L$ . Note that a finite TP with  $f'(\alpha)|_{\alpha=0,2d} \rightarrow -\infty$  implies the same infinite slope for the PDF at  $\alpha = 0, 2d$ . This is not seen in our results.